INTERNATIONAL CONFERENCE ON ENGINEERING DESIGN
ICED 05 MELBOURNE, AUGUST 15 – 18, 2005

# KINEMATIC AND CONTROL DESIGN FOR A DEXTEROUS MECHANICAL HAND

G. R. Dunlop

## Abstract

The design of a dexterous robotic hand is described. The kinematic design and the geometric optimization obtained from genetic algorithms are discussed along with a number of other issues. The hand is self contained as the actuators are contained in the palm of the hand rather than externally as is common in most robotic hand designs. The hand actuators are electric DC motors that drive the hand phalanges via direct linkages in order to avoid the friction and compliance problems of tendon drives. The direct linkage drive mechanism can encounter singularities and care is taken to avoid these singularities by careful geometric design.

Two hand designs with different sized electric motors are presented. The motor geometry for each size of motor is contained in a spread sheet, and many hand parameters and dimensions are parametrically tied to these values. The use of spread sheets to change parametric designs allows the two different hands to be generated simply by selecting the appropriate motor in the spread sheet, and by setting critical dimensions such as the phalange sizes.

*Keywords: dexterous hand, design optimization, genetic algorithms, mechatronics*

## 1. Introduction

Improvements in design and technology have resulted in less expensive robots becoming accepted by the general public, and interactions between robots, people and the human environment have increased. The robots will require dexterous manipulators that allow them to manipulate objects designed for human operation. To be aesthetically acceptable to the general public, the manipulators need to be anthropomorphic and approach the dexterity of the human hand. Robotic manipulators have already been developed for applications such as commercial domestic duties, hazardous environments (such as bomb disposal), and the complex manipulations of remote surgery [1]. The potential applications for dexterous robotic hands increase as the functionality approaches the that of the human hand.

The main types of mechanical hands that are suitable for either robot hands or human prosthetic hands are cable operated hands and linkage operated hands. Less common are pneumatic/hydraulic hands and direct drive hands that contain actuators in each joint. The design and construction of recent mechanical hands is briefly reviewed here; a more extensive review is presented by Rosheim [2].

Some initial dexterous hands have included the Salisbury Hand [3] with 9 DOF (degrees of freedom), the Utah/MIT hand [4,5] with 19 DOF, and the Belgrade/USC/SDSU hand model D-268 [6,7] with 6DOF. More recent robotic hand developments include a number of dexterous anthropomorphic robotic hands. These include the 12 DOF Robonaut hand developed by NASA [8], the 12DOF Model I [9] and 13DOF Model II [10] DLR hands, the 17 DOF NTU Hand [11], and the 24 DOF Shadow Robot hand [12].

The Stanford/JPL hand [3], and the Utah/MIT hand [4,5] are the most well known cable (tendon) operated hands. The original Stanford/JPL Salisbury hand employed rack mounted motors driving tendons to activate a 3 finger hand. The length of the Bowden cable tendons was such that compliance and friction were a problem. Despite these limitations, useful gripping and manipulation studies were conducted with the hand. The Utah/MIT hand removed most of these limitations by placing pneumatic actuators above the wrist adjacent to the hand so that all cables ran over pulleys rather than through Bowden sheaths. Thus most of the friction, and backlash problems associated with the Bowden cables were removed, but compliance remained a problem. Electric and hydraulic actuators were also investigated before the opposed pneumatic design was adopted for the Utah/MIT hand. The mark I hand had 19 DOF (degrees of freedom) and required 38 actuators. The controllers and power sources were external to the actuator package, and while the most recent Utah hand is capable of 10 beats per second (i.e. piano playing capability) it requires a 5kW air compressor to power the pneumatics [13].

Mechanically linked anthropomorphic hands are larger but do not suffer from the friction and compliance problems that plague tendon driven hands. These mechanical hands are well characterized by the Belgrade/USC hand shown in figure 1 which was the starting point for the hand described in this paper. The original Belgrade prosthetic hand [14,15] employed a fixed opposing thumb and a single electric motor to drive 4 fingers each of which closed until it made contact with the object being grasped. Once all 4 fingers had made contact, continued operation of the motor then applied equal increasing pressure to each finger via a spring loaded wiffle tree. Rather than trying to maximize dexterity and flexibility, the hand was designed for simple grasp control with the motions of the finger segments being coordinated by the built in mechanical linkages and springs responding to the grasp pressure on each finger. Thus the emphasis was on simplicity rather than individual joint control as characterized by the tendon operated hands. A second version of the hand used 4 electric motors to give improved dexterity and it is shown in figure 1a. The four fingers are coupled in pairs, and the thumb can curl and rotate into the opposed position. A further development by Vuscovik [7] is shown in figure 1b and it incorporates 2 extra electric motors for a total of 6 so that each finger is driven independently. Although the emphasis over the past decade has been on software control of the hands, these hands were the starting point for the design of the Canterbury hand which is being built in the Department of Mechanical Engineering at the University of Canterbury.

## 2. Finger Design Limitations

The finger drive mechanism of the Belgrade/USC and SDSU hands is shown diagrammatically in figure 1c. Within the palm of the hand is the DC motor driven leadscrew shown at the left hand side driving a nut. Attached to the right hand end of the palm block is the proximal (first) phalange. A driving link is attached between the top of the nut and the top of the proximal link which pivots about the center of the circle as shown. The medial (second) and distal phalanges are pivoted about their end centers as shown in figure 1b. The second driving link is attached between the top of the medial link and the lower part of the palm. This 4 bar linkage arrangement is repeated for the distal link so that movement of the proximal link via the leadscrew nut and first link results in the finger curling at the 3 finger joints. The operation of the 4 bar link is explained later when the distal drive arrangements of the Canterbury hand are discussed. However, the design has a number of problems associated with friction and backlash, effects that are greatly reduced in the Canterbury hand design which is described in the remainder of this paper.

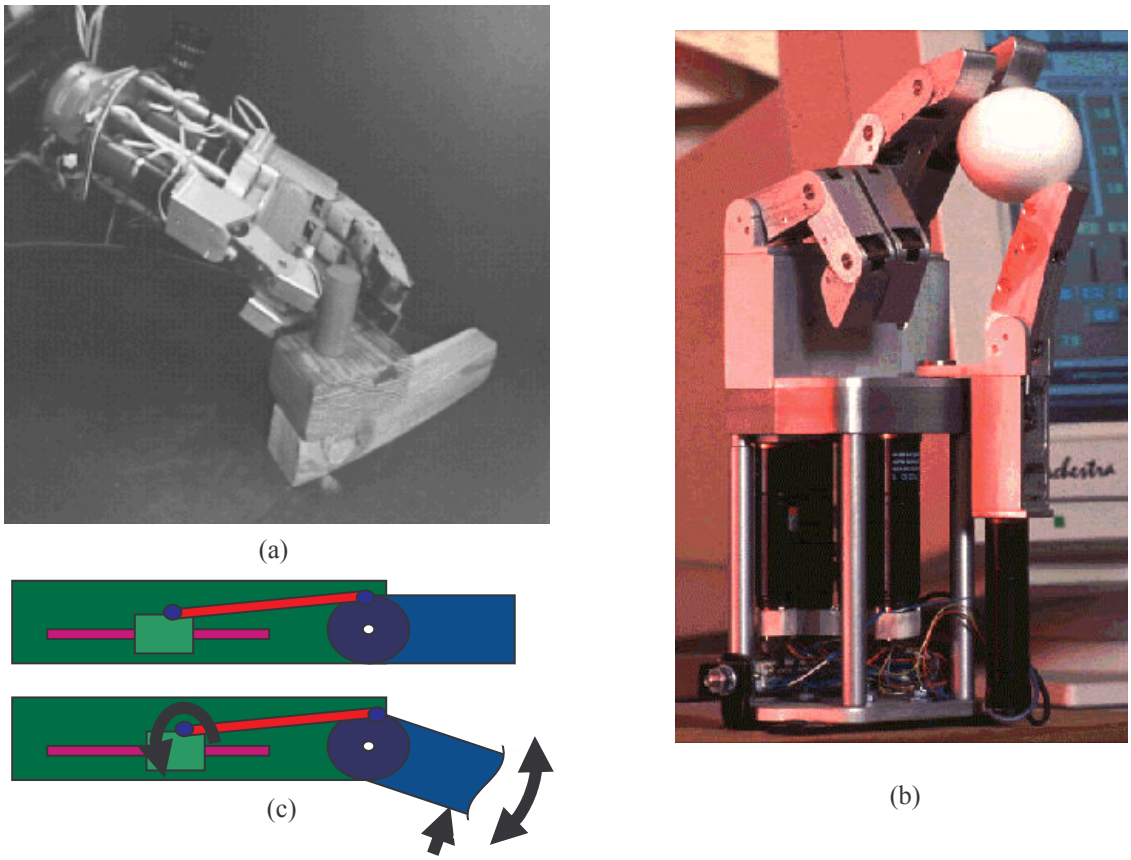

Figure 1. The Belgrade/USC/ SDSU hand driven by mechanical linkages.
(a) The mark 2 hand with 4 motors, 2 for the thumb rotation and curl, and 1 for each pair of fingers.
(b) The SDSU hand with 6 motors developed from (a) but using 1 motor for control of each finger.
(c) The hand drive mechanism is contained in each hand. The first phalange is driven by a motor – leadscrew – nut combination via a link attached to the top of the nut and the top of the proximal (first) phalange. The link force applies a torque to the nut which can jam when releasing a grasp.

## 3. Improvements

Two areas for improving the mechanical design of the Belgrade/USC/SDUC hands were identified. First the distance between the first link attachment point on the proximal link and the pivot point on the palm of the hand about which the proximal link rotates is less than half the thickness of the finger. As shown in figure 2, the design of the finger in the Canterbury hand increases this distance by moving the pivot so that the same force in the first link (actuator link 1 in figure 2) will generate a larger torque about the pivot point $P_1$. The geometry is set so that when the proximal link is in the middle of its working range, the first link is perpendicular to the radial vector $P_1P_2$ from the pivot point to the lower driving link attachment point. The geometry is set so that the torque is maximized throughout the working range i.e. the working range is spread equally about the maximum of the torque cosine curve. Thus the torque to force ratio is maximized, and the bearing load requirements reduced.

The second area of improvement was to change the attachment of the first link to the leadscrew nut. The original Belgrade/USC/SDSU finger design shown in figure 1 had the attachment point on the top of the nut so that the link forces generated a moment on the nut perpendicular to the leadscrew axis. When the finger applied maximum force to a surface, this moment (shown in the lower half of figure 1c) was often sufficient to jam the nut on the

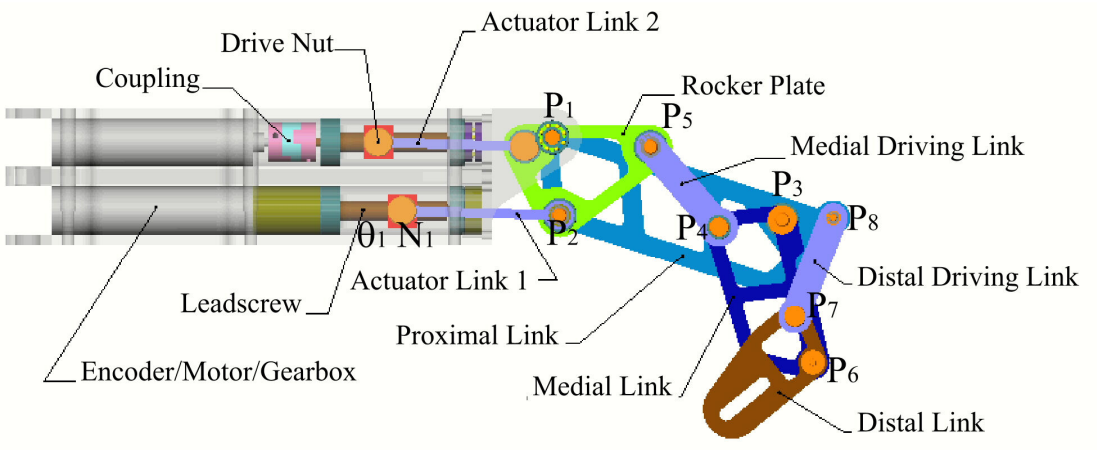


Figure 2. The original finger design for the Canterbury hand.
The lower slider-crank mechanism $\{\theta_1\ N_1\ P_2\ P_1\}$ and 2 sets of 4 bar linkages $\{P_2\ P_3\ P_4\ P_5\}$, $\{P_3\ P_6\ P_7\ P_8\}$.
Note that the upper slider-crank moves the rocker plate about $P_2$.

leadscrew and the finger could not be lifted. The improvement incorporated into the Canterbury finger design is to use 2 links on either side of the nut attached at the same level as the leadscrew axis so that a jamming moment is not be generated. Slides are incorporated on either side to react out link forces perpendicular to the leadscrew as well as to prevent nut rotation. The remaining link force component is along the line of the leadscrew axis. The resulting crosshead arrangement prevents jamming and the nut can run freely on the leadscrew.

## 4. The Canterbury hand

Once the main geometric features for an improved mechanical finger design were identified, the requirements for improved dexterity and manipulation were investigated. The balance between improved dexterity and cost is quite different for commercial prosthetic hands and experimental hands. For example, the Utah/MIT hand is very flexible but quite complex (expensive). The experimental approach is taken for the Canterbury hand in which each of the 4 fingers has 2 DOF in one plane as is shown in figure 3. All 4 fingers are spread by a single mechanism so that the plane containing each finger can be changed. Since 9 DOF are shared between 4 fingers, each finger can be considered as having 2¼ DOF.

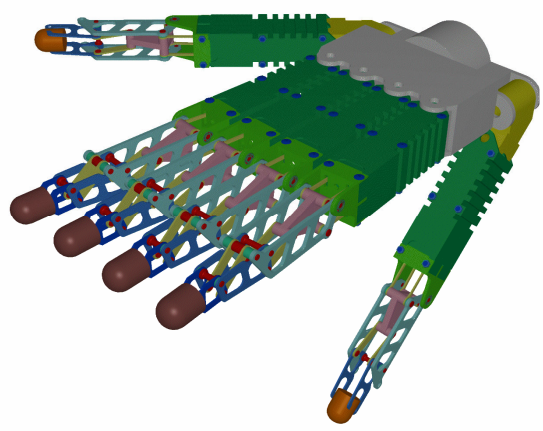

Figure 3. The original Canterbury hand design. Each finger and thumb has 2 DOF and the thumbs can also swivel into a position opposed to the fingers. Continuous manipulation is possible as 3 contact points can always be maintained on an object throughout a grasp movement.

The first Canterbury hand [16] incorporated 2 thumbs each having 3 DOF as shown in figure 3. The right thumb and the left thumb combine with the 4 fingers so that 2 sets of 3 manipulators are available for grasping objects. Static manipulation of a body requires that it be grasped at 3 points. Thus when 2 fingers and an opposed thumb reach a mechanical limit during manipulation of a body, the second set of 2 fingers and a thumb

can be brought into contact with the body to continue the manipulation as the first set of manipulators moves out of contact. Thus a grasped object can be continuously manipulated in a statically determined manner with alternating grips applied at alternating sets of 3 points.

# 5. The two DOF Finger Mechanism

Although the original Canterbury 15 DOF hand design comprised 4 fingers and 2 thumbs it was later reduced to 11 DOF using a single rotatable thumb with only 2 coupled phalanges, one being driven. In both cases the fingers used slider crank and 4 bar mechanisms as shown in figure 2. The slider-crank mechanism $\{\theta_1\ N_1\ P_2\ P_1\}$ drives the proximal phalange as shown in the figure. The slide is driven by the lower lead screw $\theta_1$. The medial phalange is operated by a 4 bar linkage $\{P_2\ P_3\ P_4\ P_5\}$. One link $P_2P_3$ is on the proximal phalange that is positioned by the lower slider-crank. The second slider-crank (upper leadscrew and actuator link 2) sets the angle of the rocker plate link $P_2P_5$, and hence the position of the medial phalange. Both slider-cranks set the medial joint position and angle. However the lower slider-crank has a relatively small effect (less than 5°) on the angle of the medial phalange, and in the NASA hand design, the rocker is renamed as the "decoupling link" [8]. The distal phalange $P_6P_7$ is also set by a 4 bar linkage $\{P_3\ P_6\ P_7\ P_8\}$ containing 2 common links on the proximal $P_8P_3$ and medial $P_3P_6$ phalanges. Thus its position is determined by the other 2 phalanges. (This mechanism is used twice in the Belgrade/USC/SDUC fingers as only the proximal phalange is driven.)

The use of this force transfer rocker mechanism was first described by Dunlop and Ward [16] and later optimized to minimise the coupling between the proximal and medial phalanges [17]. The movement of the proximal link through its 50° range results in only 3.3° of movement in the medial link. While the movements are not completely decoupled, the coupling is quite small. The distal link is coupled to the medial link so that it curls with it in the same way that the Belgrade/USC finger operates. Thus the coupling is only 6.4° in the distal link over the full movement range.

The design of the linkages and positioning of the bearings has a considerable influence on the strength and dexterity of the resulting finger. Some design constraints such as bearing load limits and the size of the finger are difficult to handle, and gradient approaches to the design are limited by the nonlinear nature of the mechanisms used. To avoid these limitations, a genetic algorithm (GA) approach was used to optimise the results presented here.

# 6. Genetic Algorithm Optimisation

Engineering design is usually a compromise as multiple objectives, some of which may be conflicting, need to be satisfied. Optimisation using numerative methods tests every point in the search space so evaluating 12 variables at 20 points per variable takes $20^{12}$ ($\sim 5*10^{15}$) design evaluations i.e. the time required is prohibitive. Another approach to design optimisation is using the usual calculus based hill-climbing methods but these require the existence of derivatives (usually a problem at mechanism singularities) and usually converge to a local maximum. Random searches may find a satisfactory design depending on luck and the number of designs evaluated, but they are no more efficient than enumerative methods. However when combined with hill-climbing methods, they can overcome the local maxima limitation and can arrive at a global maximum provided one of the random points is in the vicinity of the maximum i.e. on the same "hill".

A new search class of "natural computing" methods imitate certain principles found in nature. These include evolutionary computing, simulated annealing, and artificial neural networks [18]. Evolutionary algorithms (EAs) maintain a population of structures (possible designs) which through the process of recombination and/or mutation evolve by selecting the individual structures most suited to the environment (design criteria) and using them to breed the next generation of individuals. Genetic algorithms (GAs) are contained in this search class. It should be noted at the outset that although many of the terms used in the field of genetic algorithms have been borrowed from molecular biology, they are only simplistic analogies of the actual biological mechanisms.

A population consists of a set of individuals (possible designs), and an individual consists of a set of chromosomes, each of which in turn consists of a set of genes. The initial population can be set to random binary strings or to some known starting point (e.g. the geometry in figure 2). Each individual's genes represent encoded design variables that are used in a weighted sum to determine the fitness of an individual. The fitness of an individual determines the proportion of its genes passed to the next generation of individuals. The fitter an individual, the greater the chance that its genes will be inherited. Gene inheritance occurs when the genes of individuals are swapped to create 2 new individuals. Individuals with a high fitness can swap with many others while those with low fitness do not create any new individuals and their genetic contribution to the population dies out. Mutation of genes is used to randomly alter a percentage of the population so that some genetic outliers are created to replace lost genes or to create genes that have never existed. Thus other solutions are possible even if the population becomes relatively static. However some gene combinations may not be viable and will die out within a few generations. Disruptive random changes of genes are reduced when incremental changes are used to limit the mutation i.e. creep mutation [19]. The 5 step GA process is shown diagrammatically in figure 4.

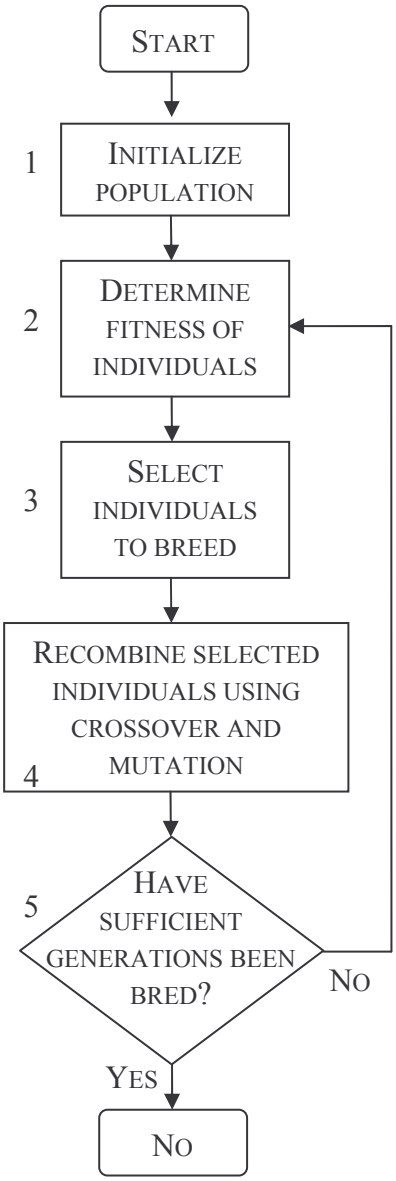


Figure 4. The Genetic Algorithm flow chart for processing successive generations of the design in order to optimize the various design tradeoffs.

Each generation of individuals is examined to determine whether to continue breeding or to halt the algorithm once a time level or degree of fit has been reached. A problem with the weighted sum fitness criteria is the lack of objectivity in assigning the weighting to each design objective because there is no a priori way to determine the sensitivity to each criterion. It was found that the GA was consistently unable to find a compromise solution and that one set of criteria was optimised at the expense of another set. Changing the weights merely altered the set membership. In another approach the design objectives are ranked and then each is optimised in the ranked order. Unfortunately, some of the genes needed for solution of lower ranked objectives were eliminated in the early stages. A hybrid scheme that set minimum levels for both ranked and weighted sum schemes

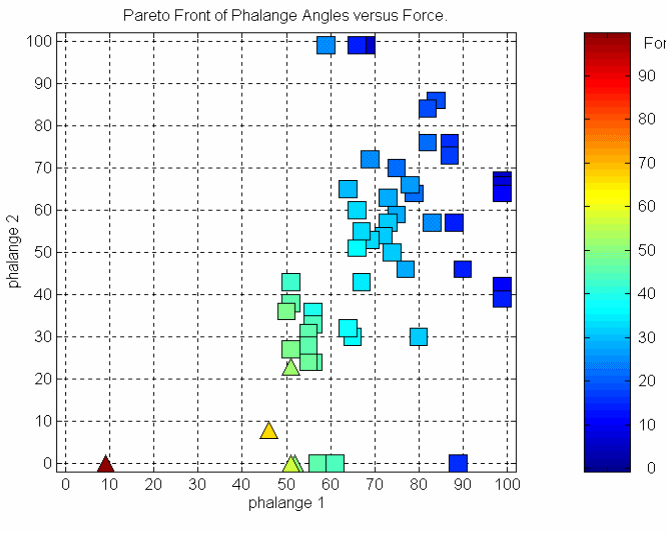


Figure 5. Each triangle and square represent an individual on the Pareto front. Code: □ < 6N and Δ > 6N. Note

clipped extreme maxima to force a compromise. However traits were still weighted and thus remained subjective.

An interesting approach to the optimal criteria problem is the Pareto Optimal set [20]. The Pareto Optimal front is the set of points on a hyper surface c.f. figure 5. The points on this hyper surface front are not less inferior to one another and cover the extreme range of each of the criteria. A problem is that individuals near extremes tend to produce less viable descendants so parent selection requires limiting the range on the Pareto front as well as the range of neighbours that can be used for interbreeding i.e. niching. Also fitness can incorporate a neighbour density weighting to thin out high density population areas so as to obtain a greater spread of design parameters. Unfortunately, as the problem dimensions increase, computation can become excessive with the result that front range limiting, neighbour and niche allocation criteria again become subjective [21] .

# 7. Design Constraints

The maximum fingertip force is computed as a function of the phalange rotation angles as it affects the dexterity and strength of the finger which are of primary concern. The coupling between the first and second phalanges is also calculated since movement in the vicinity of the singularity associated with the distal phalange 4 bar linkage can multiply the internal forces and cause damage to the bearings and links. The lead screws cannot be back driven so it is possible for large forces to be generated by one screw on the other. Due to the small amount of coupling between the phalange drivers, a "force gearing effect" can be generated, especially near the distal singularity.

To prevent interference between adjacent bearings, bearing interference was included as a fitness parameter. The GA attempts to find the bearing with the most appropriate size and strength rating but no allowance is made for sizing bearings in non-critical areas. If any members of a set of bearings are big enough to take the load and unaffected by size, then the smallest one is used. Only ball bearing races were used for this particular low friction finger design and a minimum of 1mm of metal was retained around the outer ball race housing.

The GA was programmed to minimise the knuckle thicknesses from the lower to upper finger surfaces were where possible in order to approximate an anthropomorphic hand. Using the highest of all points on the finger (i.e. highest combined joint position and bearing radius) the thickness at each knuckle was calculated by finding the lowest joint and bearing to the right of the current knuckle. Projection of the rocker above the proximal phalange was incorporated into the depth of the metacarpal/proximal joint size by considering the positions of rocker plate bearings $P_3$ and $P_5$ in both the initial straight position and while the upper lead screw was in the fully retracted position. The motor block was also included in the first knuckle thickness. The chance of converging to a solution was increased when each phalange

thickness was considered and weighted separately. Hence the fitness objectives set for the finger were:

1. Range of movement of the three phalanges was to be maximised. This was considered as three separate criteria, one for each phalange.
2. Finger tip force to be maximised.
3. Forces in connecting links minimised.
4. Phalange thicknesses to be not greater than the original finger dimensions. All three phalange thicknesses were averaged to give one criterion.
5. Coupling minimised.

The original finger sizes were used as the basis for the minimum required criteria values. Inclusion of the original finger into the initial population for small population tests showed a marked improvement in the resulting fitness of individuals. As the size of the population increases, the benefit of having the original finger in the initial population decreases. More individuals were bred before convergence and the best individuals' fitness obtained from large populations is similar to that obtained with smaller populations that started with the original finger sizes i.e. a better starting design required fewer generations for a solution.

As the population size increases the original finger genetic contribution is lessened. Hence its effect on guiding the population to individuals of similar fitness is less. Low population sizes without the original finger quickly converge to a low fitness value indicating a lack of genetic material. Higher population sizes slow the rate of convergence allowing more diverse individuals to be calculated without domination by local optima. Consequently the tests with large population sizes converge slowly to similar fitness values regardless of whether the original finger was in the initial population or not.

| **Fitness Trait** | **Fittest** | **Original** |
|---|---|---|
| Proximal Range | 58.3° | 56.1° |
| Medial Range | 65.1° | 60.0° |
| Distal Range | 89.2° | 66.6° |
| Minimum Force | 7.1N | 4.6N |
| Coupling | 4.4° | 4.8° |
| Proximal Height | 24.5mm | 27.2mm |
| Medial Height | 23.7mm | 25.4mm |
| Distal Height | 20.4mm | 21.2mm |
| Max. Link Force | 60.0N | 120.0N |

Table 1. A comparison of the original finger characteristics with those of the GA optimised finger design (shown in figure 3).

The GA developed was tested with five different initial populations of 150 individuals. Generations of 10000 new individuals were calculated to yield a "best" finger. As shown in table 1, movement range was increased from 183° to 213° mostly by movement of the distal link. The other significant improvement was increasing the minimum finger tip force by 54%. Subsequent tests indicated that, constrained to a reasonable time limit (10000 individuals taking about 18 hours), the most appropriate breeding and mutation rates were around 5%.

The Pareto plot in figure 5 shows the trade off between three traits with each phalange angle increasing at the expense of the other, and the finger tip force increasing at the expense of both angles. Phalange 1 (proximal) movement in a typical human finger or thumb is limited, so reducing the minimum trait for phalange 1 to 30 (scaled to 36°) and increasing the minimum trait for phalange 2 to 65 (distal phalange scaled to 78°) should, for a thumb, take advantage of the high force region displayed. Individual finger designs which satisfy the dimension, bearing and link force constraints are plotted as Pareto fronts for all three phalange angles and for the tip forces, and these show where further improvements are likely to be obtained.

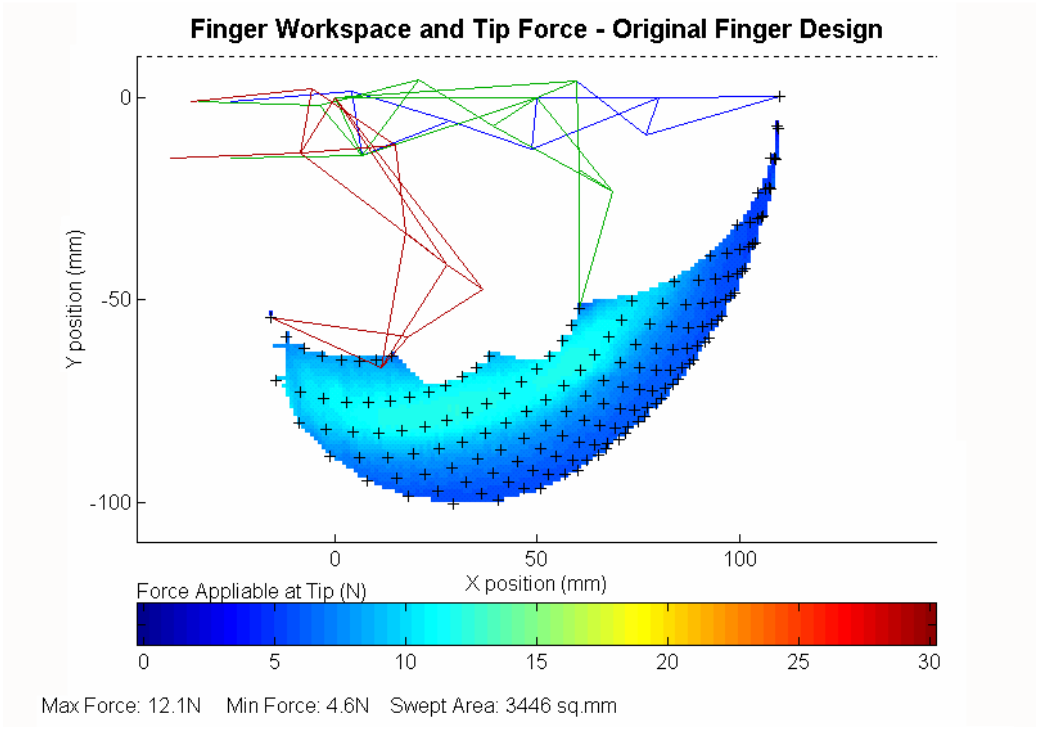


Figure 6. Force distribution throughout the finger workspace before GA optimization.

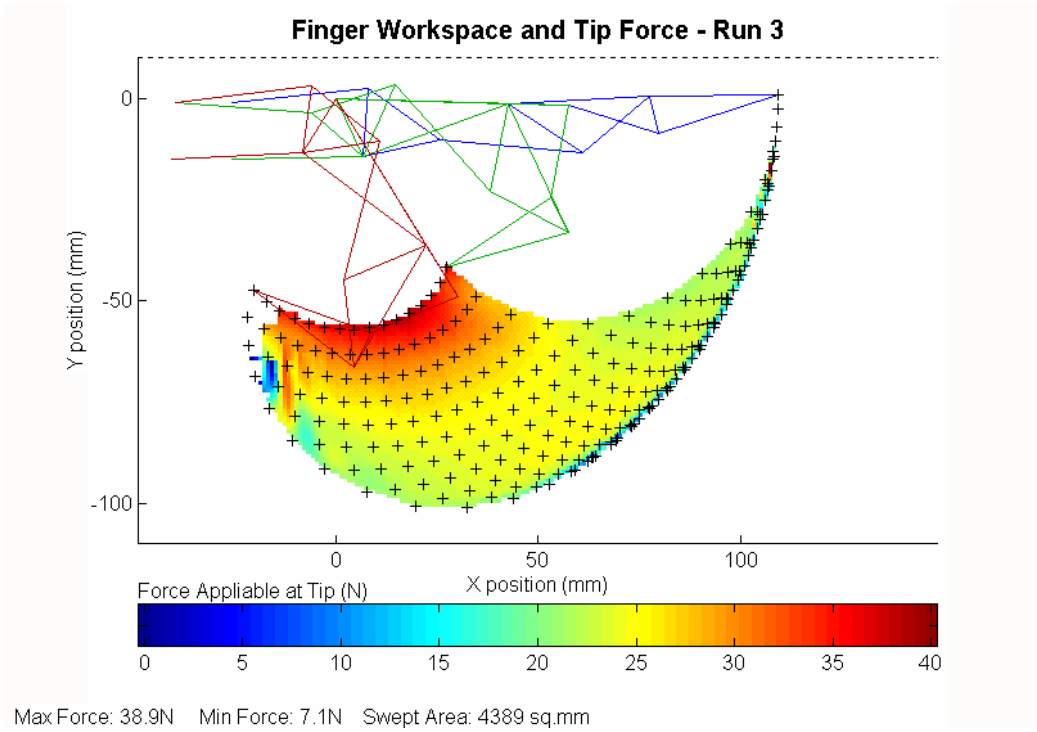


Figure 7. Force distribution throughout the finger workspace after GA optimization. Note that the working area has increased by 28% and the force available almost doubled.

The results obtained are presented as a finger workspace diagram for the first finger design and for the GA optimized design. The original finger workspace was increased by 28% and the force range almost doubled. If the workspace improvement is limited to 20% by

excluding low force areas, then the minimum force is increased by 5 times. This is a very significant improvement on what was a best manual design.

## 8. Finger Design

The motor rotation determines the geometric configuration of the various finger joints so that the grasp movements and pressures can be specified and controlled. Rather than using angle sensors at each finger joint, the shaft rotation is measured for each of the 11 DC motors so that the grasp shape and motion can be calculated from the kinematics thus providing the required hand control. Four force measurements are built in each finger as shown in figure 8, and the thumb has three.

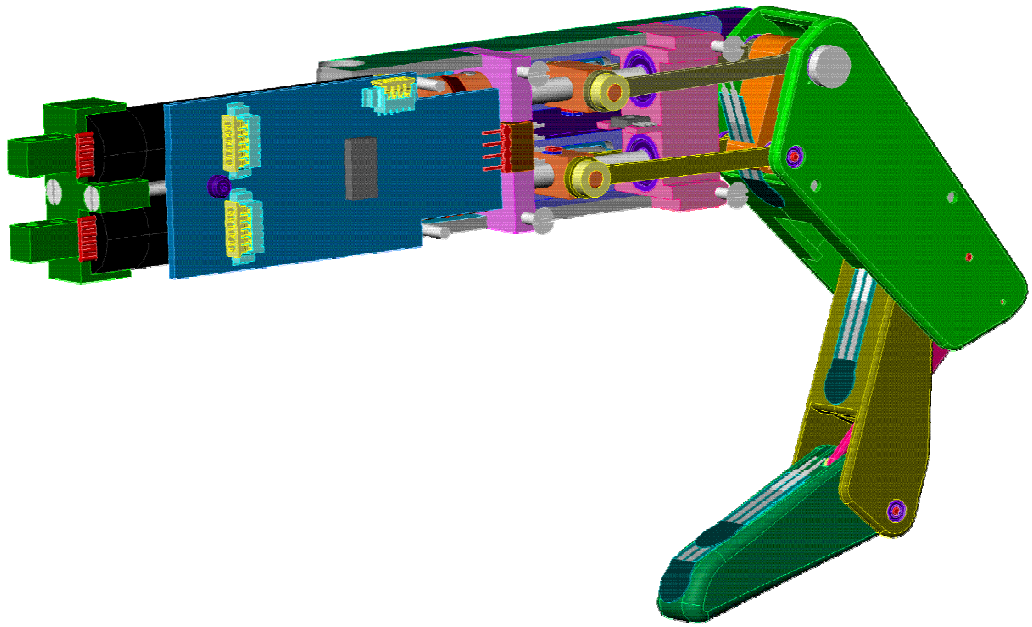

Figure 8. Cutaway view of the latest Canterbury finger construction showing the force sensing resistors fitted to the underside of the links. Note also the Hall effect sensor at the right hand end and between the lead screws. The finger control microcomputer and DC motor drives are mounted on the PCB.

Since the DC motors are incorporated in the palm of the hand, space is severely limited and there is a compromise between size, torque, speed, and heat generation. Wiring between the motors, amplifiers, sensors and controller is also minimized. A reasonable powerful computer is required for the real-time kinematic calculations and 11 DC servo feedback control loops. In excess of 100 electrical connections were needed but could not be easily incorporated in the hand. This was overcome by using a 3 wire bus around the hand, and employing 6 microcontrollers as communication nodes and for real-time servo control as well as for data measurement for each finger. The 3 wire bus is easily built into the hand and provides an 18V power supply as well as a half duplex time multiplexed multi-drop communication connection [22]. A schematic of a finger control computer is shown in figure 9.

A major design issue is heating within the hand. The 11 servo amplifiers and DC motors are enclosed in a small space so heat dissipation is important. Pulse width modulated (PWM) switching amplifiers are used to minimize heating, and an intelligent hybrid control arrangement is used to increase the efficiency of the PWM amplifiers still further. A compromise between 4 quadrant torque speed (4QTS or bipolar operation) control for acceleration and braking control, and 2 quadrant torque speed (2QTS or unipolar operation

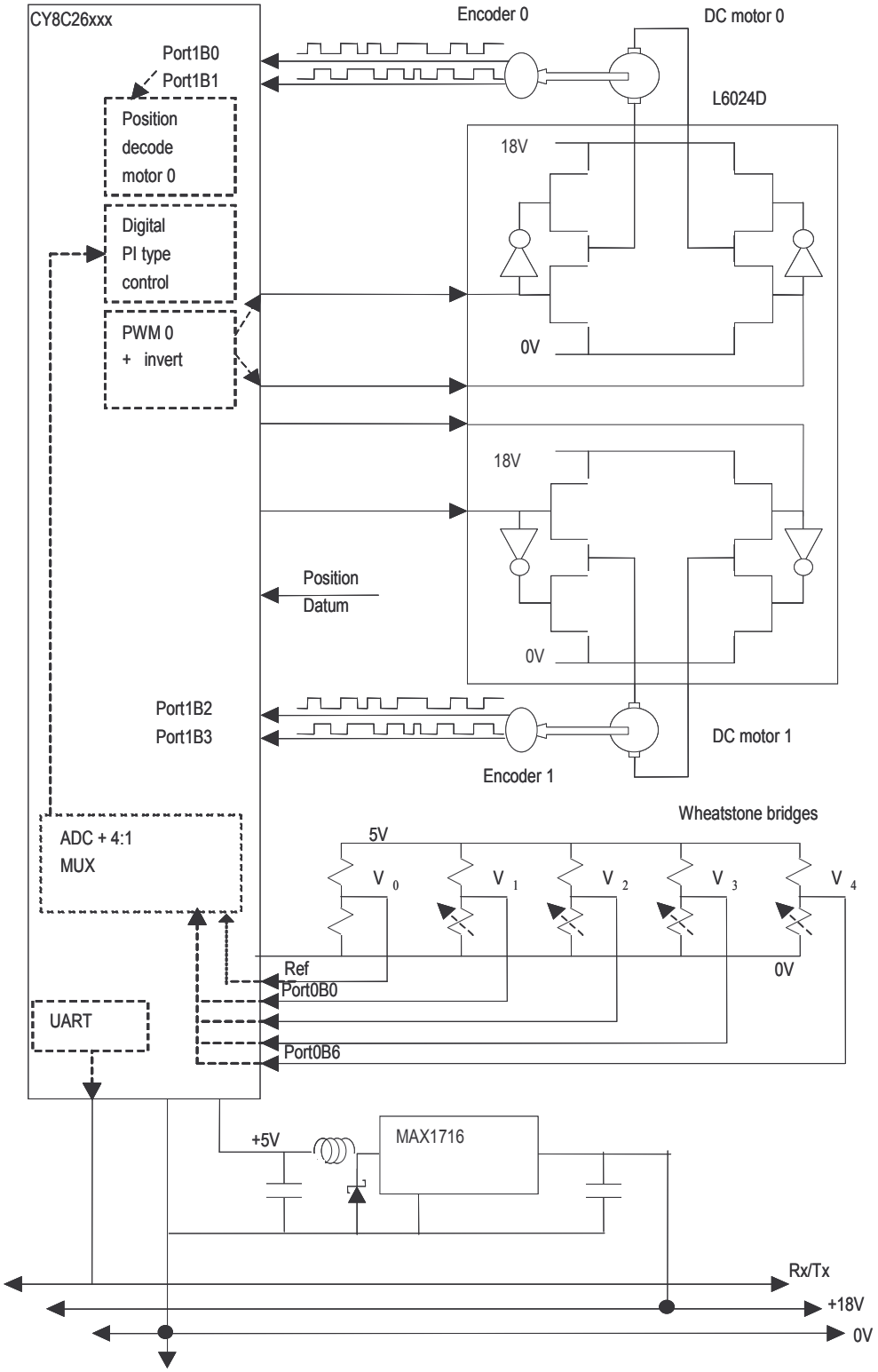


Figure 9. The microprocessor or programmable system on a chip is used in each finger to control the torque output of 2 DC motors, read the pressure on 4 sensors, and to switch from position/velocity control to force control when the finger makes contact with the object being grasped.

which is more efficient) control for acceleration only was required. A hybrid control using programmed intelligence in the microcontroller was designed so that 2QTS control is used for motoring, and 4QTS control is used for braking thus obtaining the maximum efficiency and minimizing the heating [23].

# 9. Parametric Hand Design

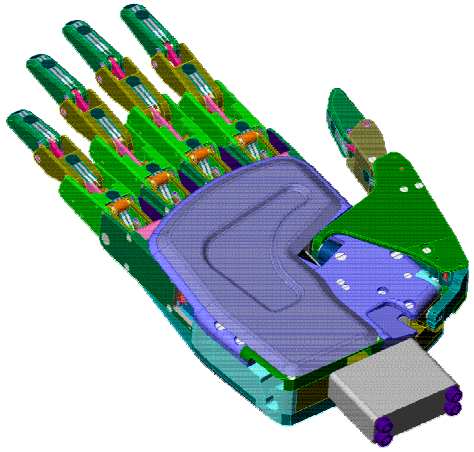

Figure 10. The optimized Canterbury hand design..

The hand is a parametric CAD design [24] so that different hands can be designed for different sized motors and fingers. This makes it relatively straightforward to generate a new set of major parts using CNC manufacturing. However, the many small parts such as shafts and spacers have been made manually on a jeweler's lathe. The parametric approach was used to generate designs for two different sized motors: a 10mm$\phi$ x 39mm 0.5W Minimotor, and a 12mm$\phi$ x 65mm 4W Maxon motor. The more powerful motor design is intended for dexterous robotic applications, while the smaller design is a prototype prosthetic unit and is currently being constructed. The smaller model is shown in figure 10. Note the circular pressure sensors on the fingers, 3 are visible and a fourth is on the finger tip. There are also another 3 large sensors beneath the cover on the palm surface. The thumb has 3 pressure sensors, and it is able to rotate about a single inclined axis within the palm.

The main objective for the CAD models is to communicate the design intent, and to allow easy modification of the motion and geometry of the hand. As well as the numerous parts for the hand there are also a large number of features in the CAD model of each hand part. Thus when making changes to the design, the hand model needs to be rebuild as quickly as possible. Several different CAD assembly structures were used for the subassemblies of the hand. Their choice depended on the function and objectives of the models. The final design structure for the models of the hand also changed over the design life cycle. Often the design began with a top down assembly method using linked parts. The references helped define parts within the assembly to make up for imperfect knowledge about the design. As the design matured and the part functions became more fully defined, the processing time became a large factor. It was then necessary to remove the references between the linked parts and subassemblies using fully defined dimensions/features. This improved both the speed and the stability of the models.

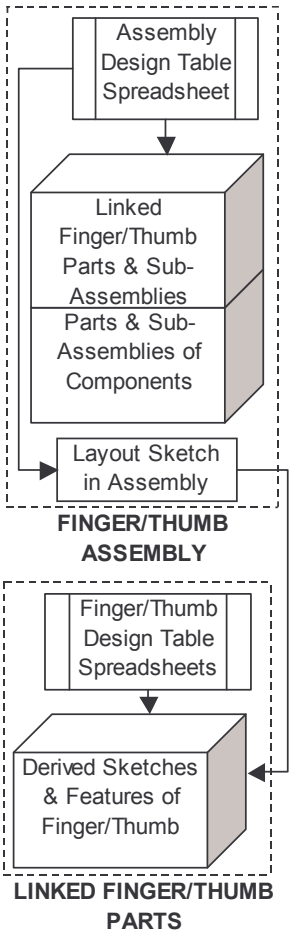


Figure 11. Linked Finger and Thumb CAD Structure.

The linked finger/thumb assembly CAD structure shown in figure 11 is much like the finger/thumb assembly structure from which it was created. It is made from two kinds of structures: components, and linked subassemblies plus finger/thumb parts. Component parts are the generic parts unaffected by the linkage bearing geometry. The linked models have geometry and features dependent on the layout sketch in the main finger/thumb assembly. The layout sketch controls the linkage model geometry, and is in turn controlled by the assembly design table spreadsheet. A typical design control spreadsheet is shown in figure 12. The design table spreadsheet also controls the configurations of the parts and subassemblies within the assembly. Any changes made to the

layout sketch causes the dependent linked models of the finger/thumb to change to match the geometry once the assembly model is rebuilt.

| | A | B | C | D | E | F | G | H | I | J | K | L | M | N | O | P | Q | R |
|---|---|---|---|---|---|---|---|---|---|---|---|---|---|---|---|---|---|---|
| 1 | **CONFIGURE** | By Christopher S. Green © 2002 | | | | | | | | | | | | | | | | |
| 2 | Hand Folder Directory | C:\users\Xris - do not delete\Solid Works 2001 Hand Files\GREEN HAND MKI | | | | | | | | | | | | | | | | |
| 3 | | | | | | | | | | | | | | | | | | |
| 4 | **FINGER (MK VI) GEOMETRY CHANGER** | **Note this Necessary Condition**: Maxon Motors (Y2 - Y1) = 14mm, and Mini Motors (Y2 - Y1) = 11mm, | | | | | | | | | | | | | | | | |
| 5 | **Canterbury Finger's X Coordinate Geometry** | Othewise the finger/thumb will not rebuild properly as they have been optimised to these conditions | | | | | | | | | | | | | | | | |
| 6 | Finger Configuration | X1 | X2 | X3 | X4 | X5 | X6 | X7 | X8 | X9 | X10 | X11 | X12 | | | | | |
| 7 | MIDDLE_MAXON | 50 | 50 | 91 | 90 | 82.5 | 108 | 127.5 | 138 | 131 | 171 | 173.5 | 210 | | | | | |
| 8 | INDEX_RING_MAXON | 50 | 50 | 91 | 90 | 82.5 | 108 | 126.5 | 137 | 130 | 169 | 171.5 | 206 | | | | | |
| 9 | LITTLE_MAXON | 50 | 50 | 91 | 90 | 82.5 | 108 | 116.5 | 126 | 120 | 150 | 151.5 | 182 | | | | | |
| 10 | MIDDLE_MINI | 50 | 50 | 89.5 | 88.5 | 82 | 103.5 | 126.5 | 136 | 130.5 | 168.5 | 170.5 | 206 | | | | | |
| 11 | INDEX_RING_MINI | 50 | 50 | 89.5 | 88.5 | 82 | 103.5 | 123.5 | 133 | 127.5 | 163.5 | 165.5 | 200 | | | | | |
| 12 | LITTLE_MINI | 50 | 50 | 89.5 | 88.5 | 82 | 103.5 | 114.5 | 124 | 118.5 | 149.5 | 151.5 | 180 | | | | | |
| 13 | | | | | | | | | | | | | | | | | | |
| 14 | **Canterbury Finger's Y Coordinate Geometry** | | | | | | | | | | | | | | | | | |
| 15 | Finger Configuration | Y1 | Y2 | Y3 | Y4 | Y5 | Y6 | Y7 | Y8 | Y9 | Y10 | Y11 | Y12 | | | | | |
| 16 | MIDDLE_MAXON | 50 | 64 | 48 | 64 | 50 | 59.5 | 50 | 50 | 56 | 51 | 59 | 51 | | | | | |
| 17 | INDEX_RING_MAXON | 50 | 64 | 48 | 64 | 50 | 59.5 | 50 | 50 | 56 | 51 | 59 | 51 | | | | | |
| 18 | LITTLE_MAXON | 50 | 64 | 48 | 64 | 50 | 59.5 | 50 | 50 | 56 | 51 | 59 | 51 | | | | | |
| 19 | MIDDLE_MINI | 50 | 61 | 49 | 62 | 50 | 57 | 50 | 50 | 56 | 51 | 58.5 | 51 | | | | | |
| 20 | INDEX_RING_MINI | 50 | 61 | 49 | 62 | 50 | 57 | 50 | 50 | 56 | 51 | 58.5 | 51 | | | | | |
| 21 | LITTLE_MINI | 50 | 61 | 49 | 62 | 50 | 57 | 50 | 50 | 56 | 51 | 58.5 | 51 | | | | | |
| 22 | | | | | | | | | | | | | | | | | | |
| 23 | **Canterbury Finger's Bearing Sizes (Determined from Outer Diameter of Bearing)** | | | | | | | | | | | | | | | | | |
| 24 | Finger Configuration | B3OD | B4OD | B5OD | B6OD | B7OD | B8OD | B9OD | B10OD | B11OD | DSL | | | | | | | |
| 25 | MIDDLE_MAXON | 4 | 4 | 7 | 4 | 4 | 4 | 4 | 4 | 4 | 27 | | | | | | | |
| 26 | INDEX_RING_MAXON | 4 | 4 | 7 | 4 | 4 | 4 | 4 | 4 | 4 | 27 | | | | | | | |
| 27 | LITTLE_MAXON | 4 | 4 | 7 | 4 | 4 | 4 | 4 | 4 | 4 | 27 | | | | | | | |
| 28 | MIDDLE_MINI | 4 | 4 | 7 | 4 | 4 | 4 | 4 | 4 | 4 | 26 | | | | | | | |
| 29 | INDEX_RING_MINI | 4 | 4 | 7 | 4 | 4 | 4 | 4 | 4 | 4 | 26 | | | | | | | |
| 30 | LITTLE_MINI | 4 | 4 | 7 | 4 | 4 | 4 | 4 | 4 | 4 | 26 | | | | | | | |
| 31 | | | | | | | | | | | | | | | | | | |
| 32 | **THUMB (MK II) GEOMETRY CHANGER** | | | | | | | | | | | | | | | | | |
| 33 | **Canterbury Thumb's X Geometry** | | | | | | | | | | | | | | | | | |
| 34 | Thumb Configuration | X1 | X2 | X3 | X4 | X5 | X6 | X7 | | | | | | | | | | |
| 35 | THUMB_MAXON | 25 | 59 | 69 | 69.5 | 100 | 100.5 | 132.5 | | | | | | | | | | |
| 36 | THUMB_MINI | 25 | 58.5 | 68.5 | 67 | 99.5 | 100 | 132 | | | | | | | | | | |
| 37 | | | | | | | | | | | | | | | | | | |
| 38 | **Canterbury Thumb's Y Coordinate Geometry** | | | | | | | | | | | | | | | | | |
| 39 | Thumb Configuration | Y1 | Y2 | Y3 | Y4 | Y5 | Y6 | Y7 | | | | | | | | | | |
| 40 | THUMB_MAXON | 65 | 51.5 | 51.5 | 61 | 51.5 | 60.5 | 51.5 | | | | | | | | | | |
| 41 | THUMB_MINI | 65 | 53 | 53 | 62 | 53 | 62 | 53 | | | | | | | | | | |
| 42 | | | | | | | | | | | | | | | | | | |
| 43 | **Canterbury Thumb's Bearing Sizes (Determined from Outer Diameter of Bearing)** | | | | | | | | | | | | | | | | | |
| 44 | Thumb Configuration | B2OD | B3OD | B4OD | B5OD | B6OD | DSL | | | | | | | | | | | |
| 45 | THUMB_MAXON | 5 | 5 | 4 | 4 | 5 | 26.5 | | | | | | | | | | | |
| 46 | THUMB_MINI | 5 | 5 | 4 | 4 | 5 | 25 | | | | | | | | | | | |
| 47 | | | | | | | | | | | | | | | | | | |
| 48 | | | | | | | | | | | | | | | | | | |
| 49 | **THUMB (MKII) AXIS GEOMETRY CHANGER** | | | | | | | | | | | | | | | | | |
| 50 | Thumb Axis Variables | X | Y | Z | MainA | SecA | TA2 | Base2 | TA1 | Base1 | StrutL | | | | | | | |
| 51 | MAXON_HAND | 58 | 29 | 52.5 | 197 | 99 | 117 | 30.5 | 100 | 20.65 | 98.5 | | | | | | | |
| 52 | MINI_HAND | 58 | 30 | 54 | 203 | 98 | 124 | 30.5 | 99.5 | 23.68 | 80 | | | | | | | |
| 53 | | | | | | | | | | | | | | | | | | |
| 54 | **HAND GEOMETRY TABLES** | | | | | | | | | | | | | | | | | |

Configure Finger

Click the Button to implement thumb changes

Configure Thumb

Click the Button to implement finger changes

Configure Axis

Click the Button to implement thumb axis changes

**Key**

Configuration = Finger/Thumb Geometry for a particular Motor Type
X1, X2, ... Xn = X Coordinate for Bearng 'n'
Y1, Y2, ... Yn = Y Coordinate for Bearing 'n'
DSL = Drive Screw Length
B2OD, B3OD, ... BnOD = Outside Diameter of Bearing 'n'
B2ID, B3ID, ... BnID = Inside (Bore) Diameter of Bearing 'n'
B2T, B3T, ... BnT = Width of Bearing 'n'
B2FD, B3FD, ... BnFD = Diameter of Flange of Flanged Bearing 'n'
B2FT, B3FT, ... BnFT = Thickness of Flange of Flanged Bearing 'n'
B2CON, B3CON, ... BnCON = Configuration Name of Bearing 'n'
X, Y, Z = Cartesian coordinate for the thumb's axis start point
MainA, SecA = Main Angle and Secondary Angle of the thumb axis
TA1, TA2 = Thumb Angle 1 and Thumb Angle 2
Base1, Base2 = Lengths of offsets at the base of TA1 and TA2
StrutL = True length of the thumb's rotation strut between the bearings

Figure 12. A typical table for setting the critical dimensions in the parametric CAD control spreadsheet.

One of the advantages of this method was the ease of control of the multiple parts in the assembly. In a bottom up design the parts would either be individually changed for the optimised geometry, or else have a program such as the spreadsheet control program make the changes automatically. Although rebuild time was a factor this method still took less time than using the spreadsheet control program. Unfortunately this method was not as stable as the bottom up assembly method if changes were made to the design of the assembly or referenced parts. Sometimes the linked parts would lose their references to the top-level design and become undefined.

The linked finger/thumb models could not have been used in the hand assembly structure, as only a single referenced geometry can be active at any time in a single part with a top down assembly structure. This would have meant the configurations could only be used in the hand assembly for non-referenced features, which reduces the parts flexibility. If on the other hand the top down method was used in the hand assembly it would require that all the fingers and their linkages be separate models.

# 10. Conclusions

The parametric design of the dexterous Canterbury hand has been presented. The unique rocker mechanism for providing a simple self contained 2 DOF finger mechanism has been described along with optimization of the design. The optimization of conflicting design requirements through the successful use of Genetic Algorithms has also been demonstrated. The computer control of the hand proved to cause many problems with all the control, power, and sensor wires being routed to a single computer so control was distributed amongst 6 smaller finger and palm control microprocessors arranged on a 3 wire bus to simply the wiring constraints. The main control computer communicates by a half duplex signal wire which is the third bus wire, the other 2 being the power supply and a ground return.

The heat generated within the hand was also considered carefully. A novel DC motor driving scheme was devised and tested with good results. The motor shaft position measurements were sufficient for velocity estimation, and thus is was possible to control the current, and hence the force output by the driving links within the finger. The control microprocessor used in each finger is actually a system on a chip so the analog multiplexers and instrumentation amplifiers needed for the force sensor measurements are contained within the microprocessor which considerably simplifies the electron circuit boards.

Finally, 2 different sized hands have been generated by the parametric CAD model and used to demonstrate a full range of grips thus confirming the dexterous nature of the design.

**Acknowledgments**

The interest and encouragement of Prof. Marko Vuskovic of SDSU who introduced the author to the Belgrade/USC hand is gratefully acknowledged. Also acknowledged are the contributions of H. Monier and L. Magnier, the project students who carried out the initial finger evaluations, and my master's thesis students, D.K. Ward who produced the first finger, A.R Bain who carried out the GA work, and C.S. Green who worked on the parametric CAD model. All have contributed to various aspects of the hand design. Finally research seed funding for this project from the University of Canterbury is also acknowledged.

**References**

[1] Minor, M., and Mukherjee, R., *A Dexterous Manipulator for minimally invasive surgery,* Proc. IEEE ICRA Int. Conf., 1999, Vol. 3, pp. 2057-2064.

[2] Rosheim, M.E., *Robot evolution: the development of anthrobotics*, New York, John Wiley and Sons, Inc., 1994.

[3] Salisbury, J. K., *Interpretation of Contact Geometry's from Force Measurements*, Robotics Research: The first International Symposium, MIT Press, 1984, pp.565-577.

[4] Jacobsen, S.C., Wood, J.E., Knutti, D.F., and Biggers, K.B., *Utah/MIT Dextrous Hand Work in Progress*, in Pham, Dr D. T. and Heginbotham, Prof. W. B., (ed.), International Trends in Manufacturing Technology – Robot Grippers, IFS (Publications) Ltd., Bedford, U.K, 1986, pp.341-389.

[5] Jacobsen SC, Iversen E K, Knutti D E, Johnson R T and Biggers K B *Design of the Utah/MIT dextrous hand*, Proc. IEEE ICRA Int. Conf., 1986, Vol. 3, pp.1520-1532.

[6] Bailon, H., Vuskovic, M.I., and Ivokovic, B. *Force Interface for the Multifingered Robotic Hand*, Proc. IEEE SMC Int. Conf., 1995, Vol. 1, pp.96-102.

[7] Vuskovic, M., Vuskovic, B., and Vuskovic, D., *Multifingered Robotic Hand D-268*, Technical Report, Robotics and Intelligent Systems Laboratory, San Diego State Univ., CA, USA, 1995.

[8] Lovchik, C.S., and Diftler, M.A., *The Robonaut Hand*: *A Dextrous Robot Hand for Space*, Proc. IEEE ICRA Int. Conf., 1999, pp.907-912.

[9] Butterfass, J., Hirzinger, G., Knoch, S., and Liu, H., *DLR's Multisensory Articulated Hand*, *Part I: Hard- and Software Architecture*, Proc. IEEE ICRA Int. Conf., 1998, Vol. 3, pp.2081-2086.

[10] Butterfass, J., Grebenstein, M, Liu, H., and Hirzinger, G., *DLR-Hand II: Next Generation of a Dextrous Robot Hand*, Proc. IEEE ICRA Int. Conf., 2001, Vol.1, pp.109-114.

[11] Lin, L.R., and Huang, H.P., *Mechanism Design of a New Multifingered Robot Hand*, Proc. IEEE ICRA Int. Conf., 1996, pp.1471-1476.

[12] Wood, R., *The Shadow Dextrous Hand/Arm*, Shadow Robot Company Ltd. URL: http://www.shadow.org.uk/products/newhand.shtml 2002.

[13] Jacobsen, S.C., Olivier, M., Smith, F.M., Knutti, D.F., Johnson, R.T., Colvin, G.E., and Scroggin, F.M., *Research robots for applications in AI, teleoperation and entertainment,* Experimental Robotics VIII, ISBN 3-540-00305-3, 2002, pp.2-21.

[14] Tomovic, R., and Boni, G., *An Adaptive Artificial Hand*, IRE Tran. AC-7, 1962, pp.3-10.

[15] Tomovic, R., and Stojiljkovic, Z., *Multi-functional terminal device with adaptive grasping force,* Automatica, 1975, Vol.11, pp.567-571.

[16] Dunlop, G.R., and Ward, D.K., *The kiematics of a fifteen degree of freedom six fingered hand*, Proc. IFToMM, 1995, Vol.3, pp.2249-2253.

[17] Dunlop, G.R., Baines, A.R, and Smaill, J.S. *Genetic algorithm optimisation of a 2 DOF finger,* Proc. IFToMM, ISBN 951-42-5289-X, 1999, Vol.3, pp.1015-1020.

[18] Heitkoetter, J., and Beasley, D., eds., *The hitch-hiker's guide to evolutionary computation* rtfm.mit.edu:/pub/usenet/news.answers/ai-faq/genetic, 1994.

[19] Davis, L., Handbook of genetic algorithms, Van Nostrand Reinhold, New York, 1991.

[20] Fonseca, C., and Fleming, P., *Genetic algorithms for multi objective optimization: formulation, discussion and generalization,* Genetic Algorithms - 5th Int. Conf., 1993, pp.416-423.

[21] Horn, J., and Nafpliotis, N., *Multi objective optimization using the niched Pareto genetic algorithm*, IlliGAL Report No. 93005, University of Illinois at Urbana-Champaign, 1993.

[22] Dunlop, G.R., *A distributed Controller for the Canterbury Hand*. Proc. Int. Conf. on Mechtronics, ICOM2003, ISBN 1 86058 420 9, 2003, pp.619-625.

[23] Dunlop, G.R., *Intelligent electric drive system – a mechatronics approach*, Proc. IEEE ICRA Int. Conf., 2003, pp.41-48.

[24] Dunlop, G.R., and Green, C.S., *CAD structure of a mechanical hand*. Proc. Int. Conf. on Computer Aided Design, CAD'04, CD Proceedings, 2004.

Dr G R Dunlop, University of Canterbury, PB4800 Christchurch, New Zealand reg.dunlop@canterbury.ac.nz